International Journal of Modern Manufacturing Technologies
ISSN 2067–3604, Vol. VIII, No. 1 / 2016

RESEARCH REGARDING FRICTION INFLUENCE OF WIRES TO JOINTS INTERIOR ON PRECISION POSITIONING OF A ROBOTIC ARM

Catalina Ciofu[1], Gheorghe Stan[2]

[1, 2] "Vasile Alecsandri" University of Bacau, Department of Industrial Engineering
Calea Marasesti, No. 157, 600115, Bacau, Romania

Corresponding author: Catalina Ciofu, blgcatalina@yahoo.com

Abstract: Robotic structures are used increasingly often in operations from industrial field. By now, designers came with innovative robotic structures that mimic the movements inspired from nature (snake, octopus arm, elephant's trunk) to achieve flexible positioning. The specific actuation of elephant's trunk robotic arms with wire-driven joints through inner structure has several important advantages such as miniaturization possibility of the robotic arm diameter, flexible positioning through narrows spaces and a large workspace with respect to robot size. Inner actuation causes elastic deformation because of wires friction to joints interior, which contributes to the decreasing of joints precision positioning. Elastic deformations of driving wires vary from joint to joint depending upon the winded surfaces number and wires length. In the analysis, we obtain variation diagrams of positioning precision for each wire driven joint on Y and Z axes. The analytical method is necessary for positioning precision optimization of the particular robotic arm.

Key words: actuating wires friction, inner actuation, serial robotic structure, precision positioning, elastic deformation.

1. INTRODUCTION

The structure of elephant's trunk robotic arms consists of serially connected joints that enable flexible spatial positioning. Joints of similar structures are commonly driven by wires or cables to actuate them from distance with actuators disposed at the base arm. This particularity assures a low weight of the robotic arm. The actuation of joints with pulley systems and driving wires placed through structure arm interior has the advantage of enabling small arm diameters along with flexible positioning in narrow spaces. However, manipulation in narrow spaces requires precision positioning that has different sources of positioning errors.

This paper highlights the influence of friction between driving wires and inner surfaces of robotic arm on positioning precision. Wire actuation of joints is commonly used at robotic hands for fingers driving as it is a demand for minimum diameters of fingers and, consequently for inner actuation with wires [1].

Robotic arms with the structure similar to elephant's trunk and a smaller number of actuators than the number of joints have motion control issues that are solved by an elastic tube mounted to arm's structure interior [2, 3, 4]. Another robotic arm similar to elephant's trunk structure has a PID device for positioning errors compensation of which sources cannot be identified, [6]. More and more researchers are developing different optimization methods of closed loop command systems and motion control using PID devices to achieve accuracy and trajectory precision of elephant's trunk robotic arms, [5, 8]. The elasticity of driving wires and their friction to joints interior surfaces entail the optimization issue of precision positioning by errors compensation of which source is elastic deformation of driving wire,s [7].

Pulley system with wires is commonly used as motion transmission mechanism of elephant's trunk robotic arms. However, wire driven joints presume positioning errors because of joints backlashes and elastic deformations of driving wires. Determination of systematic errors caused by pulley system frictions is emphasized in this paper for a particular design of elephant's trunk robotic arm with 5 degrees of freedom.

2. TRANSMISSION MECHANISM AND ACTUATION SYSTEM OF SPECIFIC JOINTS STRUCTURE

Structure design of joints C_i from the particular elephant's trunk robotic arm allows 1 degree of freedom and a rotation of angle θ_i within driving wires fixed to cylinder with of radius R_c with opposite diametrically bolts from structure interior as described in fig. 1. Each joint i (i=1...5) of the robotic arm consists of a guiding element G_i through which are crossing the driving wires of next joint i+1.

The particular joint's structure employs a specific automatic command system, fig. 2, and the crossing of

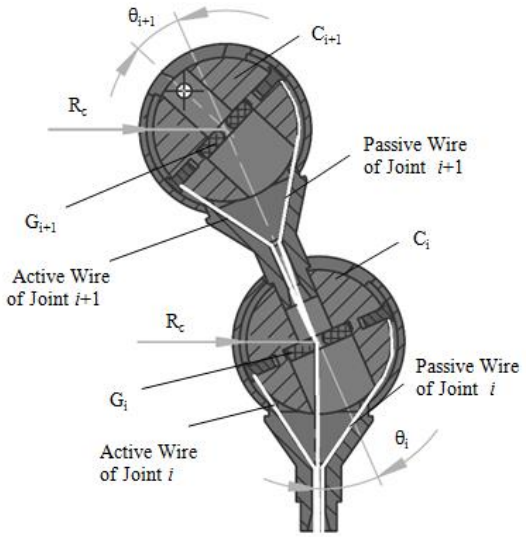

Fig. 1. The crossing of driving wires through inner joints structure of robotic arm

driving wires through robotic arm is specific to each joints. Actuating wires of joints are winding, one by one, the surfaces of radius R_2 and R_3 to which corresponds friction coefficients μ_1 and μ_2 respectively, before crossing the grooved wheel R_{ci}.

Driving mechanism of joints C_i is a tangential transmission mechanism of motion through wires and a pulley system with driving properties. Each reducer shaft r_i is linked to a grooved wheel R_{ci} which transfers the rotation to kinematic joint through two wires fixed to grooved wheel at the bottom end and to cylinder of joint (C_i) at the upper end, fig. 2. Actuation system of each degree of freedom from the elephant's trunk robotic arm consists of servomotors with variable number of revolutions (M_i), which are responsible to move a corresponding weight by a rotation motion and enable closed loop actuation. Each degree of freedom employs the rotation of different weights and a corresponding moment of inertia. The generated moments of inertia are

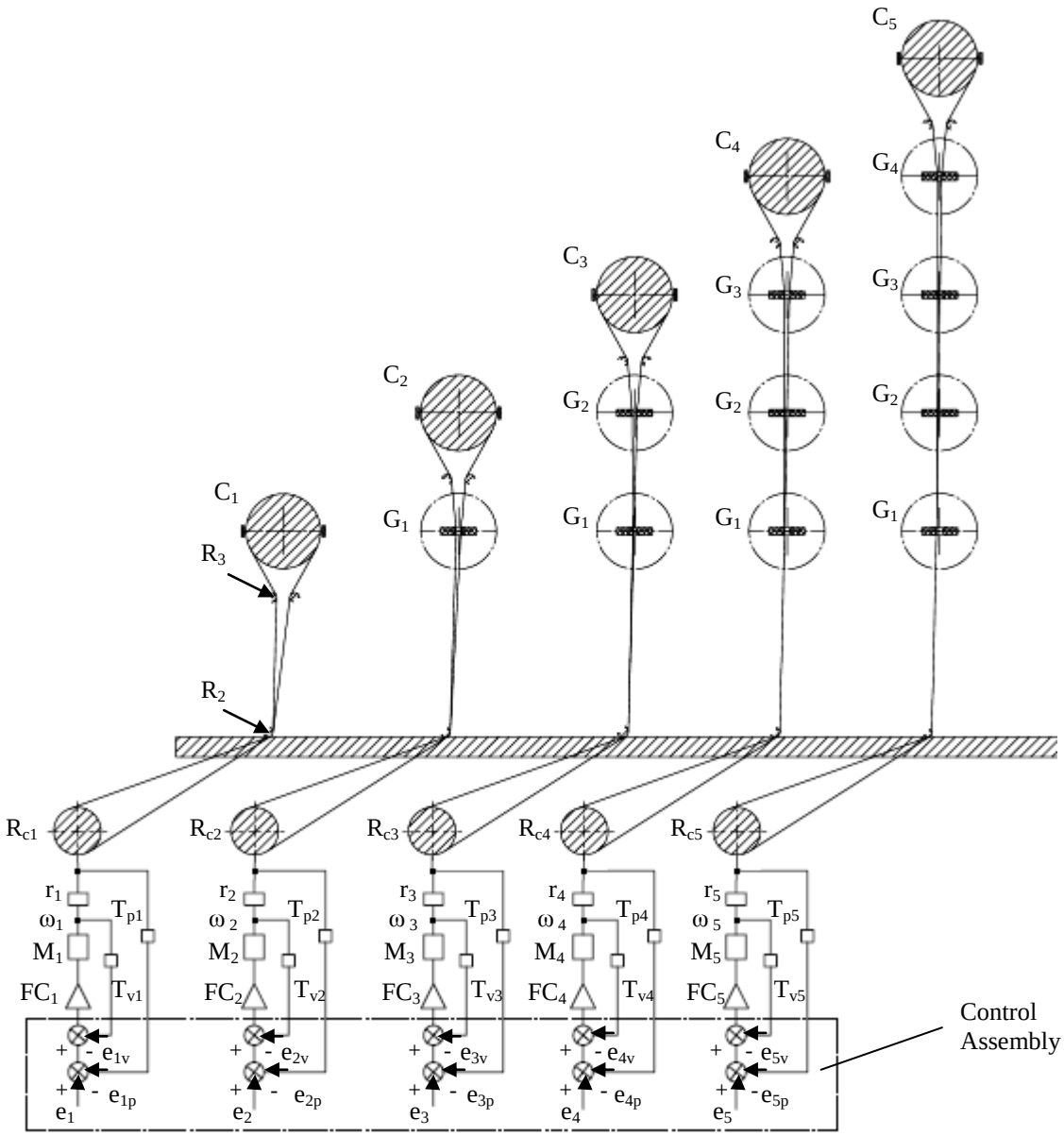

Fig. 2. The command structure of each degree of freedom

directly proportional with masses corresponding to each degree of freedom. Thus, for high masses of joints the performances of elephant's trunk robotic arm decrease.

The servo drives answer to amplifier outputs and, thus, their output is a proportional command signal given by a rotational motion ω_i and measured by a velocity transducer T_{vi} in the closed loop system.

The position of distal end robotic arm is defined by rotation θ_i of each joint i and it is controlled by the position loop with a transducer T_{pi} which is mounted on the gearbox output shaft of joint i.

Transmission of motion mechanism between gearbox shaft and universal joint shaft consist of wires and a pulley system with transmission ratio R_s / R_c. Parameters R_s and R_c define the radius of grooved wheel (R_{ci}) and the radius of joint cylinder i (C_i) respectively. Servo drives receive output signals from amplifiers FC_i (frequency converter) and give the required motion of actuation system, a rotational motion respectively.

Position transducers identify output parameters and convert them in signals accepted by the servomechanisms. Input signal of servomechanism is summed with feedback signal ($e_i - e_{ip}$) and produce the proper command signal for driving components of the system. Control assembly computes the reference parameters of servomotors M_i at each sampling period. Each joint position is controlled by the velocity loop and a digital position transducer (T_{pi}) mounted to the shaft of gearbox output, and the controlled signal is read by the assembly unit through position loop. Feedback loops enable automatic error correction of grooved wheel R_{ci} kinematic parameters (position, velocity and acceleration).

3. DETERMINATION OF PULLEY FRICTION INFLUENCE ON JOINTS POSITIONING PRECISION

The elephant's trunk robotic arm with 5 degrees of freedom and wire driven joints brings on the issue of wires friction to inner structure surfaces of joints. Friction of wires to joints interior is a sliding friction to winded circular surfaces. Driving wires are made of stainless steel with PTFE (Polytetrafluoroethylene) coating and are sliding on metallic surfaces (duralumin, steel) of robotic arm components. Friction of driving wires to circular surfaces of guiding component G_i made of PTFE, fig. 2, is ignorable because of the angle of winding about 0.122 radians and the small coefficient of friction about 0.04 [9].

The driving wires of joints subjected to friction on circular surfaces from inner structure of robotic arm presume angles of winding α_1, α_2 and coefficients of friction μ_1, μ_2 given for circular metallic surfaces with radius R_2 and R_3 respectively, fig. 3.

The effect of friction between driving wires and inner structure of robotic arm is an additional elastic deformation of driving wires on sections between angles of winding α_1 și α_2, fig. 3. Using Euler's friction equation related to wire friction we obtain equations for forces that stress additionally the driving wires, equations (1-2).

$$T' = T'' \cdot e^{\mu_1 \alpha_1} \quad (1)$$

$$T'' = T''' \cdot e^{\mu_2 \alpha_2} \quad (2)$$

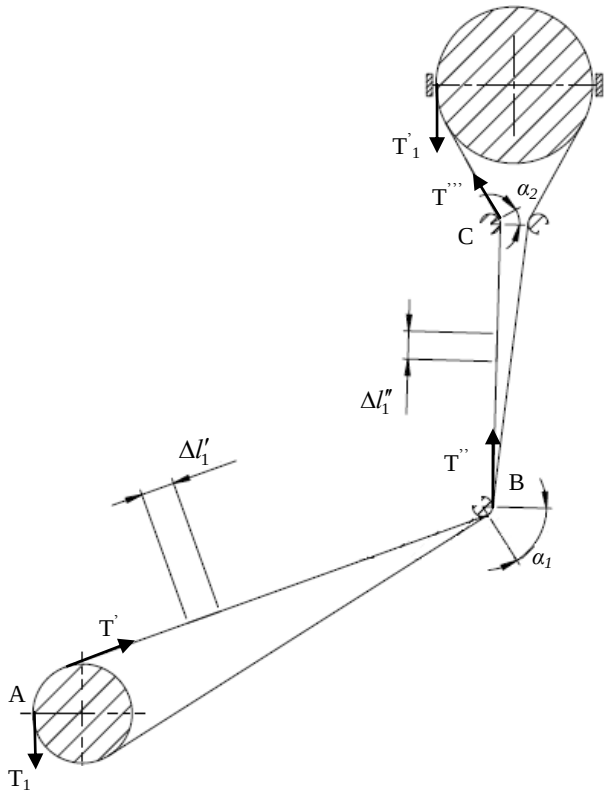

Fig. 3. Winded angles of joint driving wire

We note the pull-force applied at bottom end of driving wire with T_1 and the actuating force of joint with T_1'. From the bottom to the top end of driving wire, we note the hold-forces with T', T'' and T''', fig. 3. Therefore, with given forces and considering friction only, let us consider the following equivalences $T_1 = T'$ and $T''' = T_1'$. We obtain the relation between pull-force from bottom end of driving wire and driving force of joint using equations (1-2), equation (3).

$$T_1 = T_1' \cdot e^{\mu_1 \alpha_1 + \mu_2 \alpha_2} \quad (3)$$

Thus, actuating force of joint is smaller than the pull-force from bottom end of driving wire as given in equation (4) where we note the amount of divisor with k_i, equation (5).

$$T_i' = T_i / k_i \quad (4)$$

$$k_i = e^{\mu_1\alpha_1+\mu_2\alpha_2} \quad (5)$$

Parameter k_i given in percentage defines the coefficient of efficiency for transmission mechanism of joint *i*.

Elastic deformation of the wire Δl_1 that actuates joint *i* is the sum of elastic deformations $\Delta l_1'$ and $\Delta l''$ given for each sections length of driving wire l_i' and l_i'' respectively, equation (6), which define the length between tangent points of winded surfaces according to fig. 3.

$$\Delta l_1 = \Delta l_1' + \Delta l_1'' = (T' \cdot l_1' + T'' \cdot l_1'')/(E \cdot A_s) \quad (6)$$

$$\Delta l_i = (e^{\mu_1\alpha_1} \cdot l_i' + l_i'') \cdot T_i/(E \cdot A_s \cdot e^{2\cdot\mu_1\alpha_1+\mu_2\alpha_2}) \quad (7)$$

Using equations (1-2) and (6), we obtain equation (7) that defines elastic deformation of driving wire as a consequence of friction to joints interior *i* which depends on the value of pull-force T_i applied at wire end fixed to groove wheel R_{ci}.

Length l_i' defines the section length of driving wire between grip point A on grooved wheel and tangent point B after winding circular surface with angle α_1.

Length l_i'' defines the section of driving wire between tangent point B and tangent point C after winding circular surface with angle α_2.

Elastic deformations of driving wires entail positioning precision of joints issue and, thus, angular deviations, equation (8).

$$\Delta\theta_i = (180 \cdot \Delta l_i)/(\pi \cdot R_c) \quad (8)$$

Angular deviations of joints affect positioning precision of distal end robotic arm and entail positioning errors because the pulley system is not part of closed loop command system.

If we substitute the known structural and kinematic parameters into equation (8) we obtain the influence of friction between driving wires and interior structure of robotic arm on precision positioning of joints.

Friction coefficients depend on the surface quality between PTFE coated stainless steel wire and interior of joints structure, the surfaces roughness of mating metals respectively. The elephant's trunk robotic arm consist of metal components with specific roughness R_a=1.6 of circular surfaces from structure interior that are winded by driving wires upon radius R_2 and R_3, fig. 2.

Therefore, for the specific structure of elephant's trunk robotic arm we have friction coefficients given in table 1. The lengths of driving wires before elastic deformation, l_i, the lengths of driving wires sections subjected to friction, l_i' and l_i'', the angles of friction to inner circular surfaces of robotic arm structure, α_1 and α_2, are also constructive given.

In real case each driving wire of joints from elephant's trunk robotic arm with 5 degrees of freedom are subjected to different pull-forces T_i.

Table 1. Structural parameters

		C_1	C_2	C_3	C_4	C_5
μ_1 μ_2		0.10 0.08	0.10 0.08	0.10 0.08	0.10 0.08	0.10 0.08
α_1 α_2	[rad]	0.9774 0.5411	0.9774 0.4189	0.9774 0.4189	0.9774 0.4189	0.9774 0.4189
l_i	[*mm*]	204	254	304	354	404
l_i' l_i''	[*mm*]	113.64 59	113.64 109.15	113.64 159.15	113.64 209.15	113.64 259.15

In the analysis, we use the same value T_i = 1 *N* for all *i* pull-forces applied in order to achieve the amount of joints positioning errors proceeded from friction between driving wires and structure interior of robotic arm.

The radius of cylinder joint and the radius of grooved wheel are also constructive given, R_c=16 *mm* and R_s=10 *mm* respectively. Maximum rotation on X axis of universal joints *i* is θ_i=±23° in both directions. In calculus we consider that joints are rotating in left direction by pulling the active wire as shown in fig. 3, and, thus, the angle of joints rotation is θ_i=23°.

We also know: cross sectional area of driving wires A_s=0.113 mm^2 and Young modulus *E*=252523.55 *MPa*. Thus, we determine the ratios T_i / T_i' given by parameters k_i in table 2.

Using equations (7) and (8) we obtain elastic deformations of the 5 driving wires and rotation deviations of joints respectively, as a consequence of friction to circular surfaces from inner structure of elephant's trunk robotic arm, table 2.

Table 2. Elastic deformations and resulted positioning deviations

		C_1	C_2	C_3	C_4	C_5
$k_i \cdot 100$	[%]	96.07	96.30	96.30	96.30	96.30
Δl_i	[μm]	5.1184	6.5111	7.8997	9.2882	10.6768
$\Delta\theta_i$	[´]	0.335	0.4262	0.5170	0.6079	0.6988

From table 2 we find that friction of driving wires to inner structure of joint 1 and of subsequent joints reduce the efficiency of transmission mechanism with maximum 3.93 % and 3.70 % respectively. The difference of 0.23 % between last mentioned efficiencies comes from the value of angle α_2 different at joint 1. Elastic deformations of driving wires are about micrometers and do not exceed 10.7

μm at the wire that actuates joint 5.

The variation of positioning errors for each joint depends on angular deviations $\Delta\theta_i$ and results from the positioning equations obtained with homogeneous transformation matrices. Let us consider the world coordinate system $O_iX_iY_iZ_i$ of joint *i*, fig. 4, with position coordinates x_i, y_i and z_i, which define nominal position of joint *i*, equation (9), towards base coordinate system $O_0X_0Y_0Z_0$, $(x_0, y_0, z_0) = (0, 0, 0)$ respectively.

For the analysis, let us assume the position of previous joints in the zero position reference in order to achieve deviations of joints that arise only from friction between driving wires and inners surfaces of robotic structure, equations (16-17).

$$\begin{bmatrix} 0 \\ 0 \\ 0 \\ 1 \end{bmatrix} = \begin{bmatrix} 1 & 0 & 0 & 0 \\ 0 & \cos\theta_i & -\sin\theta_i & 0 \\ 0 & \sin\theta_i & \cos\theta_i & i \cdot l \\ 0 & 0 & 0 & 1 \end{bmatrix} \cdot \begin{bmatrix} x_i \\ y_i \\ z_i \\ 1 \end{bmatrix} \quad (9)$$

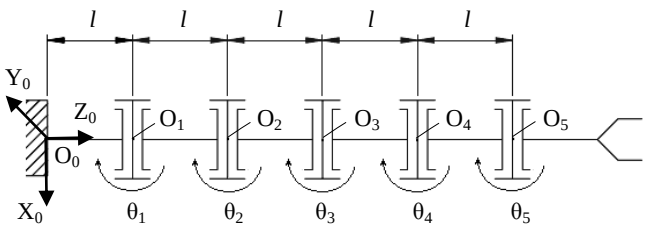

Fig. 4. Elephant's trunk robotic arm kinematics

We note the distance between joints with *l*, fig. 4. From equation (9) we obtain nominal position x_i, y_i and z_i of joint *i* given by equations (10-12) towards the base coordinate system of robotic arm depending upon rotation angle θ_i.

$$x_i = 0 \quad (10)$$

$$y_i = -i \cdot l \cdot \sin\theta_i \quad (11)$$

$$z_i = -i \cdot l \cdot \cos\theta_i \quad (12)$$

The rotation of joints on X axis entail that position coordinate x_i equals with zero at each joint *i*. We obtain virtually position of joints on Y and Z axes by adding angular deviations $\Delta\theta_i$ into positioning equations of each joint, equations (13) and (14) respectively.

$$y_i' = -i \cdot l \cdot \sin(\theta_i + \Delta\theta_i) \quad (13)$$

$$z_i' = -i \cdot l \cdot \cos(\theta_i + \Delta\theta_i) \quad (14)$$

The absolute difference between virtual and nominal positions on Y and Z axes define absolute positioning errors, equation (16) and (17) respectively.

$$\Delta y_i = |y_i' - y_i| \quad (16)$$

$$\Delta z_i = |z_i' - z_i| \quad (17)$$

Fig. 5 and fig. 6 highlight the variation of positioning errors on Y and Z axes respectively. Positioning errors of joints reach variable values about micrometers that are due to friction between driving wires and inner surfaces of robotic arm.

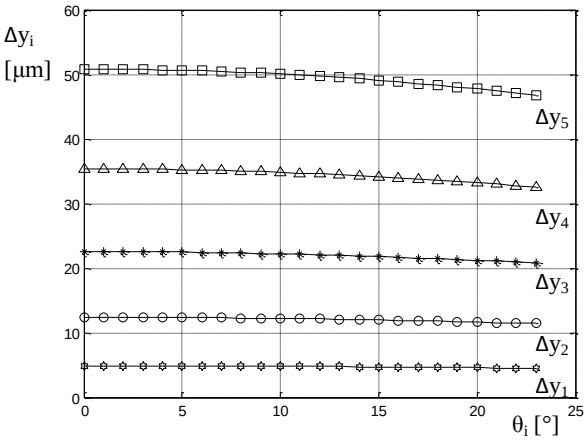

Fig. 5. Diagram of positioning errors on Y axis

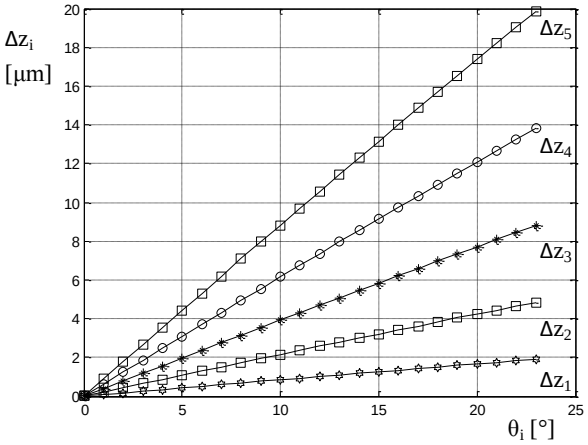

Fig. 6. Diagram of positioning errors on Z axis

The maximum positioning errors are obtained at driving wire of joint 5 that are about 50μm and 20μm on Y and Z axes respectively. From variation diagrams of positioning precision, we find that positioning errors from Y axis decrease as the angle of rotation increase because of cosine function.

4. CONCLUSION

The elephant's trunk robotic arm with 5 degrees of freedom, wire driven universal joints through inner structure and wire-pulley system presume friction of

driving wires to joints interior issue. The rotation of joints on X axis only implies positioning errors about micrometers on Y and Z axes, Δy_i and Δz_i respectively. In the analysis, we obtain that friction between driving wires and inner surfaces of robotic arm affects also the efficiency of pulley system and goes to minimum 96%.

Driving mechanism of the elephant's trunk robotic arm include AC servomotors that actuate the wires in a closed loop system. Thus, elephant's trunk robotic arms may reach minimized diameters and adequate precision of spatial positioning.

However, positioning errors resulted from elastic deformation of driving wires due friction to inner structure of robotic arm are found outside the closed loop system and presume the use of compensation methods. The obtained elastic deformations reach about 5μm at driving wire of joint 1 and 10μm at driving wire of joint 5. These deformations affect precision positioning of joints and imply maximum rotation deviation about minutes of sexagesimal degrees, 0.335´ at joint 1 and 0.6988´ at joint 5. The rotational deviations cause positioning errors that reach maximum 50μm at the zero position of joint 5 on Y axis.

We obtained positioning errors of joints without taking into consideration the positioning deviation of previous joints and, thus, we assumed in the analysis that previously joints to the analyzed joint are in zero position. We recommend the obtained results for further research of maximum positioning errors at end-effector using the positioning equation from direct kinematics when all previously joints reach maximum rotation.

Elastic deformations considered as an effect of driving wires friction to inner structure surfaces of joints are a part of total elastic deformations supported by the driving wires of joints from considered elephant's trunk robotic arm. Additionally to the analyzed deformations, there are elastic deformations from resistance moments of each joint. Therefore, for a complete analysis on precision positioning of robotic arm we have to take into consideration both mentioned sources that affect elastic deformations of driving wires.

Positioning errors obtained in this paper are systematic errors that are generally adjusted by adequate correction applied in the programming algorithm of robotic arm to eliminate positioning deviations obtained in analytical and experimental research.

5. REFERENCES

1. Lewis, F. L., et. al., *End effectors and Tooling*, "Robotics" Mechanical Engineering Handbook, (1999), Ed. Frank Kreith, pp. 29, CRC Press LLC, Boca Raton.

2. Li, J., Xu, C., Yao, Y., Ding, J., Fang, H., (2015), *Predicting synchronous accuracy of the wire sheave drives*, Precision Engineering, 39, 261-269.

3. Li, Z., Du, R., (2013), *Design and Analysis of a Bio-Inspired Wire-Driven Multi-Section Flexible Robot*, Int J of Advanced Robotic Systems, 10, 209 – 220.

4. Liao, B., Li, Z., Du, R., (2012), *Robot Tadpole with a Novel Biomimetic Wire-driven Propulsor*, Proceedings of the 2012 IEEE Int Conf on Robotics and Biomimetics, 557 – 562, Guangzhou, China

5. Heidari, S., Piltan, F., Shamsodini, M., Heidari, K., Zahmatkesh, S., (2013), *Design New Nonlinear Controller with Parallel Fuzzy Inference System Compensator to Control of Continuum Robot Manipulator*, Int J of Control and Automation, 6 (4), 115 – 134.

6. Sadrnia, O. R., Piltan, F., Jafari, M, Eram, M., Shamsodini, M., (2013), *Design PID Estimator Fuzzy Plus Backstepping to Control of Uncertain Continuum Robot*, International Journal of Hybrid Information Technology, 6 (4), 31 - 48.

7. Song. S., Li, Z., Yu, H., Ren, H., (2015), *Shape reconstruction for wire-driven flexible robots based on Bézier curve and electromagnetic positioning*, Mechatronics, 29, 28 – 35.

8. Xiong, Y., Li, Y., (2015), *Modified Internal Model Control Scheme for the Drive Part with Elastic Joints in Robotic System*, J Intell Robot Syst, 79, 475 – 485.

9. Available from: http://www.engineeringtool box.com/friction-coefficients-d_778.html, Accesed: 15/04/2016.

Received: December 10, 2015 / Accepted: June 10, 2016 / Paper available online: June 20, 2016